Proceedings of the ASME 2013 32nd International Conference on Ocean, Offshore and Arctic Engineering
OMAE2013
June 9-14, 2013, Nantes, France

OMAE2013-10735

A PROBABILISTIC METOCEAN MODEL FOR MOORING RESPONSE IN GULF OF MEXICO HURRICANES

Jan Mathisen
Det Norske Veritas
Høvik, Norway

Torfinn Hørte
Det Norske Veritas
Høvik, Norway

ABSTRACT

Hindcast data for a specific location is utilised to develop a joint probability function for the metocean variables that are expected to have a significant effect on mooring line tensions for a floating platform moored at that location. The main random variables comprise: peak significant wave height, peak wind speed, peak surface current speed, peak wave direction, peak wind direction and peak current direction, where "peak" indicates the maximum intensity of the metocean effect during a random hurricane. The time lead of peak wind relative to peak waves and the time lag of peak current after peak wind are included as random variables. It is also necessary to describe the time variation around the peak events. Simple models are assumed based on inspection of the time variations during severe hurricanes. Only the part of the hurricane during which the significant wave height exceeds 80% of the peak value is taken into account. The duration of this interval is included. Linear variation is assumed for the directions, hence the rates of change of the 3 directions are included. A linear (triangular) plus parabolic model is assumed for the time variation of the intensities of the 3 metocean effects around their respective peaks. A single parameter is required to define the proportion of linear and parabolic models for each effect and the values of this parameter for each of the 3 metocean effects are also included as random variables.

A random hurricane can be drawn from this metocean model, such that the time variation of the metocean actions is deterministic once the values of the random variables have been selected. The overall duration of the hurricane is split into short intervals, each of 15 minutes duration, such that stationary response may be assumed during each short interval. The extreme value distribution of line tension during each short interval is obtained. These distributions are combined to obtain the extreme distribution of line tension during the hurricane. Second order reliability methods are applied to integrate over the distribution of the metocean variables and obtain the distribution of extreme tension during a random hurricane. The annual frequency of hurricanes is used to derive the annual extreme value distribution of line tension.

The model is intended for the reliability analysis of the ultimate limit state of mooring lines, but may also be applicable to other response variables. The present paper is primarily concerned with the metocean model, but it is intended to include sample results for the extreme line tension.

INTRODUCTION

Probabilistic metocean models are commonly applied in response analysis of mooring systems in Norwegian waters, for use in structural reliability analysis [1]. The moderate rate of change of metocean conditions during a storm at these latitudes permits the common assumption of 3 hours duration of each realization of short-term, stationary, metocean conditions. Metocean conditions tend to change more quickly during a hurricane in the Gulf of Mexico, such that 3 hours duration for the most severe conditions during a hurricane may be an over-conservative assumption. It is also difficult to determine the most severe conditions a priori, since peak wind, peak wave and peak current conditions do not necessarily coincide. A probabilistic model is developed here to describe the variation of metocean conditions through the course of a hurricane as a set of relatively short, stationary states, and to compute the distribution of line tension, taking account of all these states.

The present model includes fitted distribution functions for wind, wave and current variables, thus facilitating detailed insight into the metocean conditions associated with extrapolation beyond the range of observed conditions. Such insight is not possible when extrapolating the distribution of response from response analysis for observed conditions only, as described by Tromans and Vanderschuren [2]. Furthermore, increasing non-linearity of response with the severity of the metocean conditions, beyond observed conditions, can be explicitly included in the response analysis.

Distributions for the metocean variables are fitted to hindcast data for a particular location in the Gulf of Mexico. Hence, extrapolation to long return periods is dependent on the

adequacy of this data. More generalized models for hurricanes, including the effect of the distance of a platform location from the hurricane path as described by Wen [3] and by Toro et al [4] should be able to make better use of the overall hurricane data, but with some increase in complexity.

NOMENCLATURE

For random variables, upper case represents the random variable itself and lower case represents a realisation.

a_Z, b_Z	parameters of Gumbel distribution for line tension.
a_0, a_1, a_2	coefficients of model functions.
A_L, a_L	coefficient of linear part of shape function.
A_P, a_P	coefficient of parabolic part of shape function.
$f_X(x)$	probability density of variable X.
$F_X(x)$	cumulative distribution function of variable X.
H, h	significant wave height.
H_p, h_p	peak significant wave height.
H_d, h_d	duration of hurricane above 80% of peak sign.wave ht.
t	time.
T_p, t_p	spectral peak wave period.
U, u	surface current speed.
V, v	1-hr average wind speed at 10m above sea level.
V_d, v_d	duration of hurricane above 80% of peak wind speed.
X, x	general variable.
Z, z	extreme mooring line tension
α_X	scale parameter in Weibull distribution of X.
β_X	shape parameter in Weibull distribution of X.
γ_X	threshold parameter in Weibull distribution of X.
Θ, θ	vector of variables defining hurricane conditions.
ψ	vector of variables defining short-term conditions.
v	hurricane frequency

METOCEAN DATA

Hindcast metocean data from GOMOS08 [5] is used, for the years from 1950 to 2008. Data are provided at 15-minute intervals. Data from 3 adjacent grid points (35055, 35067, 35079) were available, in deep water (951 to 2521 m depth), all at latitude 28.1875n and longitude from 87.75w to 89.25w. Thus, these grid points are about 83 km apart in the East-West direction. A total of 201 tropical storms and hurricanes are included in the hindcast, but all these tropical cyclones do not necessarily affect the present grid points to a significant effect. Although all the data do not originate from hurricanes, we will still use the term hurricane for convenience, and because events above a suitable threshold are mostly expected to stem from hurricanes.

A sample time history of the most severe hurricane at one grid point is shown in Figure 1 and Figure 2. The abscissae of both figures show the time after the event of the peak significant wave height; i.e. the maximum significant wave height during the hurricane.

The ordinate axis of Figure 1 is normalised relative to the peak value of each effect (wave height, wind speed, current speed) and the maximum value of the (spectral) peak wave

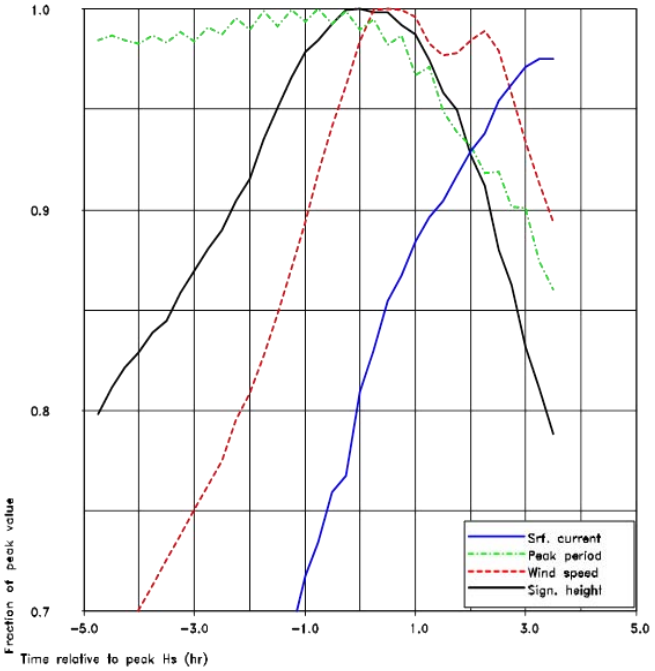

FIGURE 1 RELATIVE MAGNITUDES AROUND PEAK OF 1ST STORM FROM GRID POINT T8035055: PEAK H=15.95M AT 2005.08.29, PEAK V=45.0M/S, MAX T_P=15.7S, PEAK U=2.41M/S.

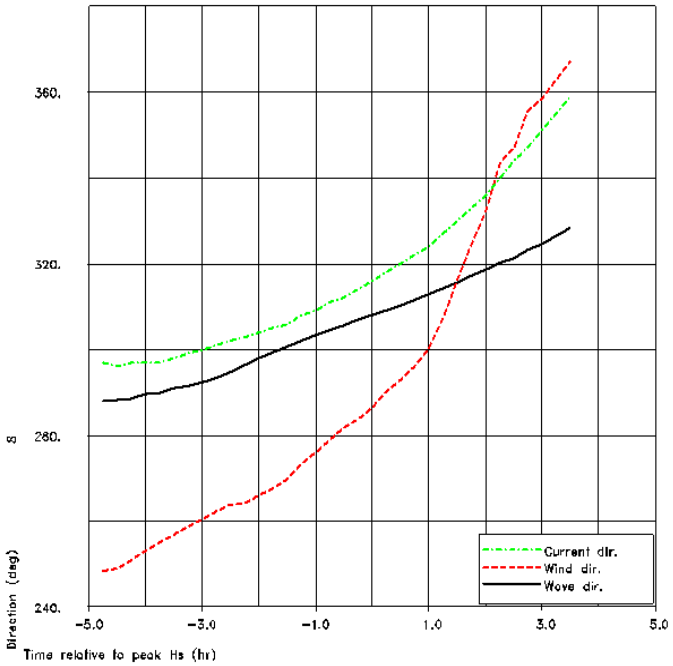

FIGURE 2 DIRECTIONS AROUND PEAK OF 1ST STORM FROM GRID POINT T8035055.

period. This normalisation is applied to allow several effects to be shown on the same figure and to gain an impression of the shapes of the time variation curves around the peak events. In this instance, the peak wave event slightly leads the peak wind event, whereas the opposite is perhaps more typical. The wind speed shows two local maxima, but the reduction in speed in

the trough between these maxima seems relatively small, presumably less than expected from passage of the eye of the hurricane. The lag of the peak current after peak waves and wind is fairly typical. The directions on the ordinate axis of Figure 2 are compass directions towards which the metocean effects are headed.

SHAPE FUNCTIONS

Intensity of metocean effects

The shapes of the time histories of several of the most severe hurricanes at all 3 grid points were plotted and studied. A simple approach to generalise and randomise these shapes was sought. The entire time history of a hurricane is not required, only the part that contributes significantly to the distribution of the maximum value of the response that is being considered. The simplest shape function appropriate to the intensities of the wave, wind and current effects could be a symmetric, linear rise and fall, as in an isosceles triangle. The next option could be a parabolic function, allowing more time in the vicinity of the peak event. A combination of these two functions was selected and referred to as a linear plus parabolic shape function. This function for the time variation of the significant wave height can be expressed as

$$h(t) = h_p\left[a_L\left(1 - 0.4\left|\frac{t}{h_d}\right|\right) + a_P\left(1 - 0.8\left(\frac{t}{h_d}\right)^2\right)\right], \quad -\frac{h_d}{2} < t < \frac{h_d}{2} \qquad (1)$$

where $a_L + a_P = 1$ and the numeric coefficients in this expression are chosen to give 80% of the peak height at both ends of the interval.

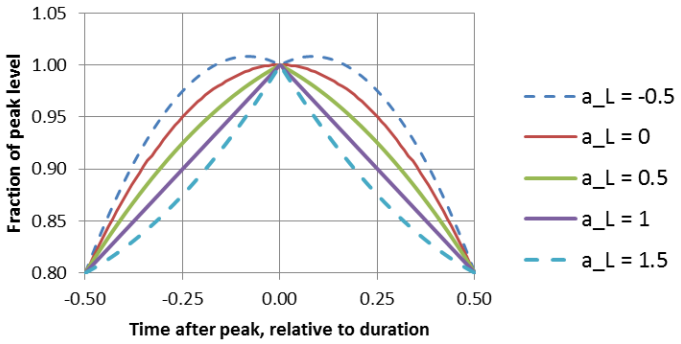

FIGURE 3 BEHAVIOUR OF LINEAR PLUS PARABOLIC SHAPE FUNCTION FOR DIFFERENT VALUES OF THE LINEAR SHAPE PARAMETER a_L.

This set of shape functions is illustrated in Figure 3. The dashed curves apply to coefficients somewhat outside the range originally expected, but still provide a behaviour which is not too unreasonable, although negative values lead to double peaks that exceed the specified peak level. An alternative approach to the time variation of wave conditions using Slepian models may be found in [13].

A procedure is arranged to estimate a_L as the single parameter required for the linear plus parabolic shape function from the data. The fit is based on approximate equality of the sum of the squares of the observed values at 15 minute intervals, while above the threshold defined at 80% of the peak value. Other procedures could be considered. Resulting estimates of the linear shape parameter from the data are shown in Figure 4 for the wave height and in Figure 5 for the wind speed. Conditional mean values and standard deviations are also included in these figures.

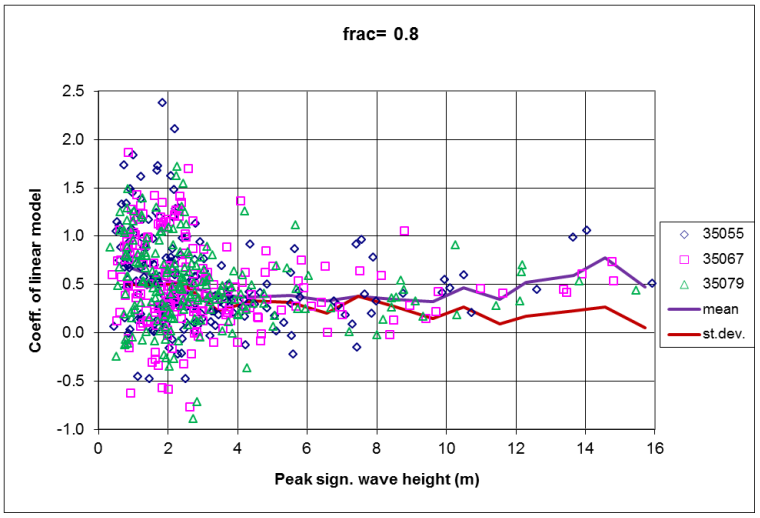

FIGURE 4 COEFFICIENT a_L OF SHAPE FUNCTION FOR SIGNIFICANT WAVE HEIGHT.

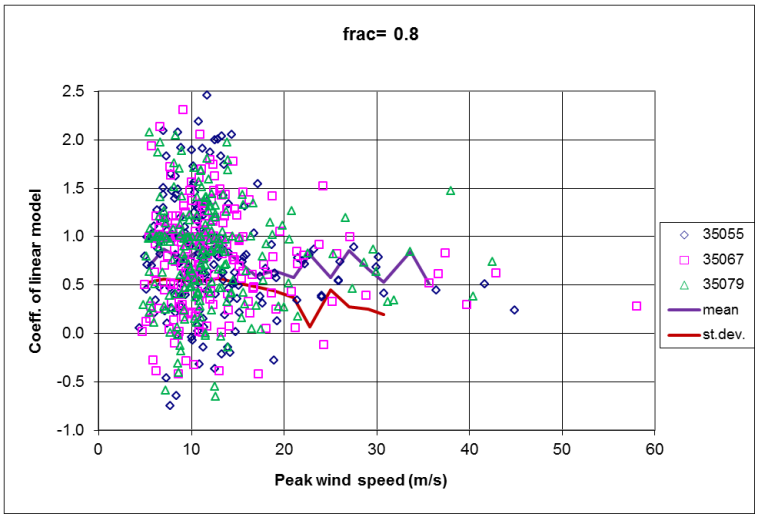

FIGURE 5 COEFFICIENT a_L OF SHAPE FUNCTION FOR WIND SPEED.

For severe peak conditions, the estimated parameter tends to lie within the intended range from 0 to 1, while much more scatter is seen for milder conditions. The trend with peak conditions has been investigated, but it does not seem worthwhile to include such trend as part of the model. Hence, it is suggested that the coefficients for waves and wind can simply be modelled as Gaussian random variables with mean

values and standard deviations taken from the results above the threshold levels, as listed in Table 1. Note that the mean value of the linear shape parameter is larger for wind speed than for wave height, indicating shorter duration of the wind speed near the peak value.

TABLE 1 STATISTICS OF LINEAR SHAPE PARAMETER FOR SIGNIFICANT WAVE HEIGHT AND WIND SPEED.

	Significant wave height A_L	Wind speed A_L
Mean value	0.41	0.64
Standard deviation	0.27	0.35

The shape of the current variation is much less symmetrical about the peak value, such that the linear plus parabolic model does not seem directly applicable. However, the rising current speed seems to follow the rising wave height quite well, with some time lag. Hence, the shape function for the wave height is also applied to the current speed, with a suitable time lag. It is assumed that the contribution of the metocean states with falling current speed to the distribution of the mooring line tension is relatively insignificant, such that the excessively rapid fall-off in speed with this model is unimportant. (The shape function for current is changed later.)

Wave period and directions

Simpler, linear shape functions are applied to the time variation of the other metocean variables. For the peak wave period, the rate of change is determined in two parts: prior to the peak significant wave height and after the peak significant wave height. For the directions of the metocean effects, the average rate of change is taken from the entire interval while the intensity of that effect is above 80% of its peak value. In use, the linear models for directions are centred on the respective peak directions; i.e on 3 different time instants, in general.

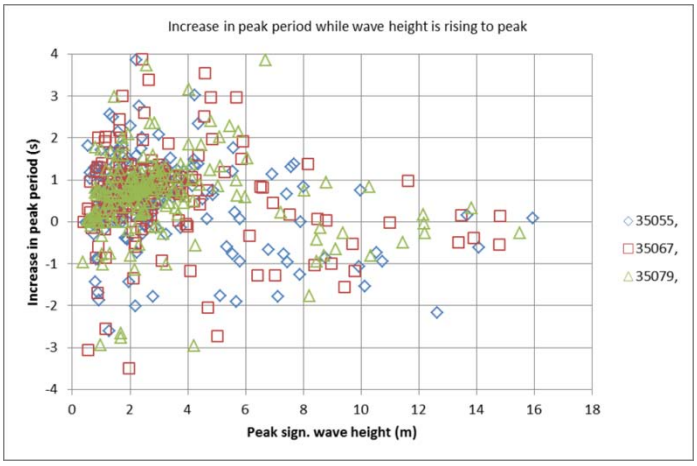

FIGURE 6 SCATTER PLOT OF INCREASE IN PEAK WAVE PERIOD WHILE THE SIGNIFICANT WAVE HEIGHT IS RISING, PLOTTED AGAINST PEAK SIGNIFICANT WAVE HEIGHT IN A HURRICANE, FOR 3 GRID POINTS.

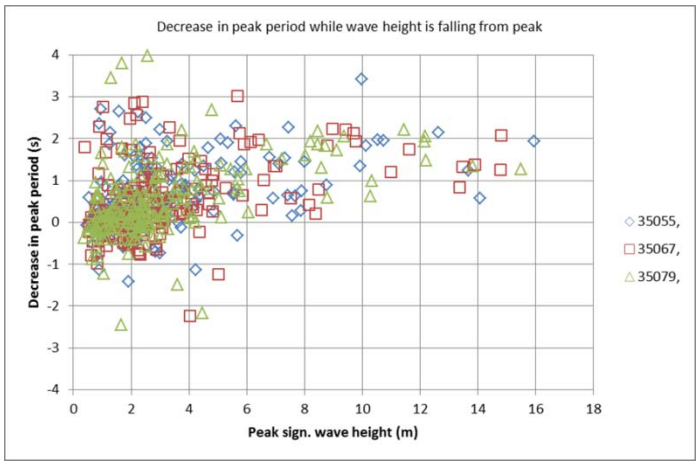

FIGURE 7 SCATTER PLOT OF DECREASE IN PEAK WAVE PERIOD WHILE THE SIGNIFICANT WAVE HEIGHT IS FALLING, PLOTTED AGAINST PEAK SIGNIFICANT WAVE HEIGHT IN A HURRICANE, FOR 3 GRID POINTS.

Results for the peak wave period are shown in Figure 6 and Figure 7. In severe conditions, the changes in period are relatively small. On average, the period actually falls while the height is increasing and while the height is decreasing, somewhat more in the latter case.

Reasonable trends with increasing peak height are found for the changes in peak wave period, so model functions are fitted to these trends. Two simple functions are utilised: a power function expressed by

$$x(h_p) = a_0 + a_1 \cdot {h_p}^{a_2} \quad \textbf{(2)}$$

and an exponential function expressed by

$$x(h_p) = a_0 + a_1 exp\{a_2 h_p\} \quad \textbf{(3)}$$

The parameters of the model functions for the decrease in peak wave period are listed in Table 2.

Results for rates of change of wave, wind and current directions are shown in Figure 8 to Figure 10. Corresponding statistics are listed in Table 3.

The rates of change are assumed to be Gaussian random variables, with the parameters provided in Table 2 and Table 3.

TABLE 2 COEFFICIENTS OF MODELS FOR DECREASING PEAK WAVE PERIOD WHILE SIGNIFICANT WAVE HEIGHT IS ABOVE 0.8 OF THE PEAK SIGNIFICANT WAVE HEIGHT – FOR HEIGHT IN METRES.

Coefficient	Mean decrease during rising wave height (s)	Std.dev. of decrease during rising wave height (s)	Mean decrease during falling wave height (s)	Std.dev. of decrease during falling wave height (s)
Model type	Con-stant	Exponen-tial func.	Power func.	Exponen-tial func.
Constant term a_0	0.3	0.1	0	0.383
Linear factor a_1	---	2.34	0.649	2.14
Exponent or exponential factor a_2	---	-0.117	0.349	-0.266

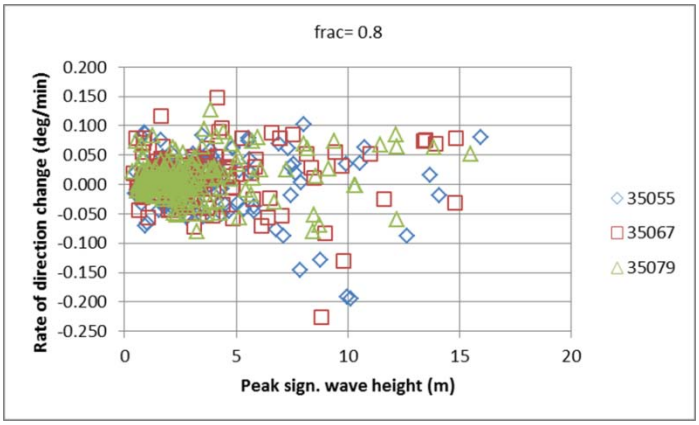

FIGURE 8 SCATTER PLOT OF RATE OF CHANGE OF WAVE DIRECTION AND PEAK SIGNIFICANT WAVE HEIGHT, FROM 3 GRID POINTS.

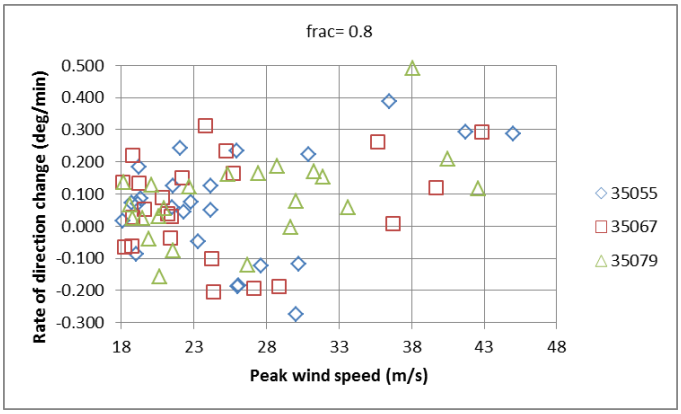

FIGURE 9 SCATTER PLOT OF RATE OF CHANGE OF WIND DIRECTION AND PEAK WIND SPEED, FROM 3 GRID POINTS, FOR WIND SPEEDS ABOVE THE THRESHOLD.

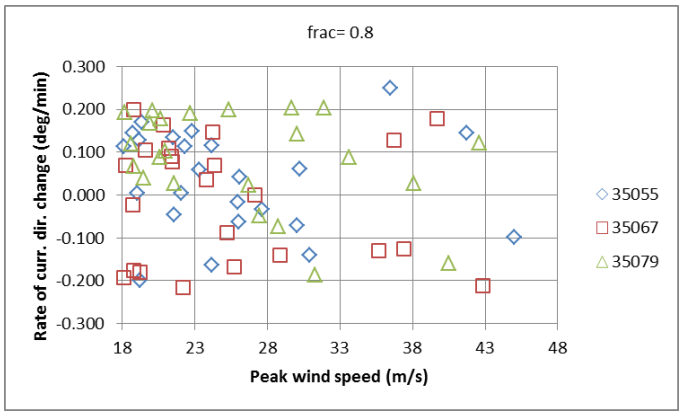

FIGURE 10 SCATTER PLOT OF RATE OF CHANGE OF CURRENT DIRECTION AGAINST PEAK WIND SPEED FROM 3 GRID POINTS, FOR WIND SPEEDS ABOVE THE THRESHOLD.

TABLE 3 RATES OF CHANGE OF WAVE, WIND AND CURRENT DIRECTIONS IN DEG/MIN.

	Rate of change of wave dir.	Rate of change of wind dir.	Rate of change of current dir.
Mean value	-0.01	0.10	0.03
Standard deviation	0.10	0.21	0.13

PEAK INTENSITIES

The procedures applied to the peak intensities are more familiar and are only briefly described. Weibull distribution functions are assumed applicable to the peak significant wave height, the peak wind speed and the peak current speed. Distribution parameters are estimated from the pooled data for the three grid points using a maximum likelihood approach. Threshold levels of 6m for the peak significant wave height and 18.8 m/s for the peak wind speed are applied. Only 21 or 22 hurricanes are included at each grid point with these threshold levels, giving a hurricane frequency of 0.356 per year. Hence, it seems appropriate to include uncertainty in the Weibull parameters in a reliability analysis. The maximum likelihood approach provides a basis to estimate this uncertainty, but it is omitted here for brevity. Statistical uncertainties could also be considered with respect to the shape functions, but they are judged to be less important.

The three-parameter Weibull distribution may be written as

$$F_X(x) = 1 - exp\{-\left(\frac{x-\gamma_X}{\alpha_X}\right)^{\beta_X}\} \quad \textbf{(4)}$$

The estimated parameters of the marginal distributions are listed in Table 4. It is important to take account of the dependencies between these variables. The Nataf approach [6] is applied here. The following correlation coefficients are estimated from the data for the normalised variables above the threshold levels:

- 0.81 between peak significant wave height and peak wind speed,
- 0.77 between peak wind speed and peak current speed.

A more detailed dependency between waves and wind might be desirable, as applied by Bitner-Gregersen and Haver [7], but this type of model may be difficult to apply when the amount of data is small.

TABLE 4 DISTRIBUTION PARAMETERS FOR PEAK WAVES, WIND AND CURRENT.

	Peak sign. height H_p (m)	Peak wind speed V_p (m/s)	Peak current speed U_p (cm/s)
Scale parameter α_X	3.95	8.88	51.9
Shape parameter β_X	1.36	1.05	1.20
Threshold parameter γ_X	6	18.8	75

A conditional log-normal distribution is applied for the peak wave period coincident with the peak significant wave height. In the present case, the model functions for the parameters are fitted directly to the conditional mean and standard deviation of the peak wave period, rather than to mean and standard deviation of the logarithm of the period. The parameters of the model functions are listed in Table 5.

TABLE 5 COEFFICIENTS OF MODELS FOR MEAN VALUE AND STD. DEVIATION OF PEAK WAVE PERIOD (IN SECONDS) AS A FUNCTION OF PEAK SIGNIFICANT WAVE HEIGHT – FOR HEIGHT IN METRES.

Coefficient	Mean of peak wave period	Std. dev. of peak wave period
Model type	Power function	Exponential function
Constant term a_0	0.0	0.340
Linear factor a_1	5.83	9.51
Exponent or exponential factor a_2	0.356	-0.400

TIME DURATION

The time duration while the significant wave height is above 80% of its peak value is extracted from the data for each hurricane. Similarly, the time duration while the wind speed is above 80% of its peak value is extracted, too. Scatter plots of these durations are shown in Figure 11and Figure 12. A trend towards shorter durations with increasing severity is apparent in both cases. Hence, exponential model functions are applied to capture these trends in the conditional mean values and standard deviations. Conditional Gaussian distributions are assumed for both time durations and the estimated parameters of the corresponding model functions are listed in Table 6. The time duration of the current speed is not required, since the shape function for wave height is applied to model the shape of the current variation with time.

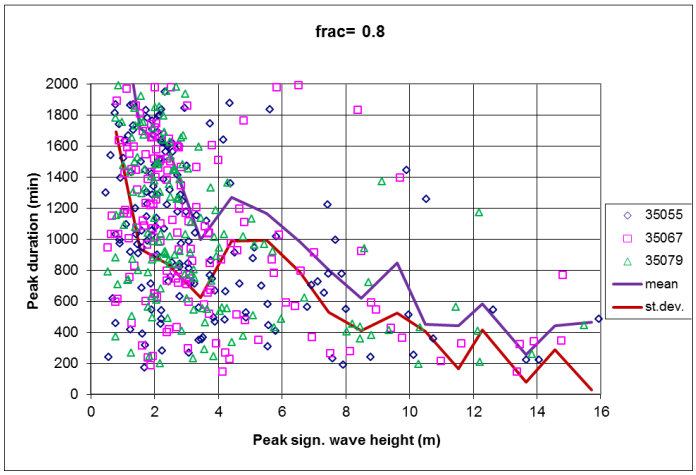

FIGURE 11 SCATTER PLOT OF TIME DURATION H_d ABOVE 0.8 OF PEAK VALUE AGAINST PEAK SIGNIFICANT WAVE HEIGHT FROM 3 GRID POINTS.

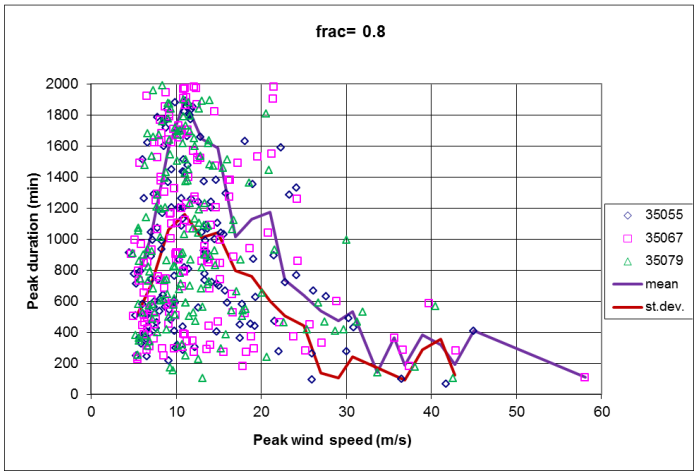

FIGURE 12 SCATTER PLOT OF TIME DURATION V_d ABOVE 0.8 OF PEAK VALUE AGAINST PEAK WIND SPEED FROM 3 GRID POINTS.

TABLE 6 COEFFICIENTS OF EXPONENTIAL MODELS FOR MEAN VALUE AND STD. DEVIATION OF TIME DURATIONS ABOVE 0.8 OF PEAK SIGN. WAVE HEIGHT AND PEAK WIND SPEED

	Wave duration h_d (function of peak ht. h_p in m)		Wind duration v_d (function of peak speed v_p in m/s)	
Coefficient	Mean (min)	Std.dev. (min)	Mean (min)	Std.dev. (min)
Constant term a_0	279	30	60	30
Linear factor a_1	2580	2410	3450	2330
Exponential factor a_2	-0.207	-0.191	-0.0669	-0.0701

TIME OFFSETS

Wind lead

The time lead of peak wind speed before peak significant wave height is extracted from the data and shown in Figure 13. For low wave heights, the wind peak tends to lead the wave peak in the majority of cases. This tendency is not equally obvious as the wave height increases. It seems sensible to consider the ratio of the lead time to the storm duration for modelling purposes – to avoid unrealistically long lead times in comparison with storm durations. The conditional ratio of lead time to duration of significant wave height above 80% of the peak value is considered. From these results, it seems reasonable to assume that the mean lead time is zero under severe conditions, while the fitted model for the standard deviation can be used to allow for some randomness in the lead time. An exponential model, as in equation **(3)**, is applied for the ratio of the lead time to the duration and the fitted coefficients are:

$a_0 = 0.0086,\ a_1 = 0.75, a_2 = -0.14.$

A Gaussian distribution is assumed.

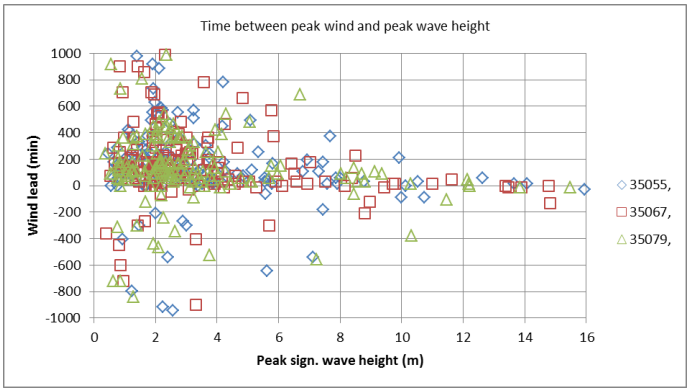

FIGURE 13 SCATTER PLOT OF TIME LEAD OF PEAK WIND SPEED BEFORE PEAK SIGN. WAVE HEIGHT AGAINST PEAK SIGN. WAVE HEIGHT FOR 3 GRID POINTS.

Current lag

The time lag of peak current speed after peak significant wave height is extracted from the data and plotted against the corresponding peak values of significant wave height in Figure 14. It appears that the peak current speed does not necessarily lag the waves or wind in moderate conditions. However, in severe conditions, this scatter diagram confirms that the peak current tends to arrive some time after the peak waves. Plausible trends with severity are not found, so it is assumed that the current lag after peak waves may simply be modelled as a Gaussian random variable with:

- mean value = 209 minutes,
- standard deviation 177 minutes.

DIRECTIONALITY

Wave directions

The wave direction simultaneous with the peak significant wave height during a hurricane is here referred to as the peak

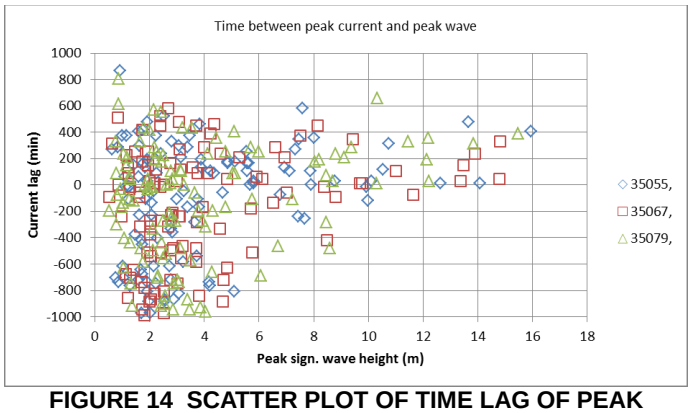

FIGURE 14 SCATTER PLOT OF TIME LAG OF PEAK CURRENT AFTER PEAK SIGN. WAVE HEIGHT AGAINST PEAK SIGN. WAVE HEIGHT FOR 3 GRID POINTS.

wave direction (not to be confused with the direction of the peak wave energy in a directional wave spectrum). The vector mean direction of the waves provided in the hindcast data is taken as the wave direction, defined as the direction towards which the waves are travelling, clockwise from North. Peak wave directions are extracted from the data set. A scatter plot of peak wave directions and peak significant wave heights is shown in Figure 15. The range of the wave directions is adjusted so that it is approximately centred on the mean of the peak wave directions.

The circular mean peak direction [8] above the threshold significant wave height of 6 m is estimated to be 301.2°. The corresponding arithmetic mean, using angles from the adjusted range, is 301.8°, which is near enough. Figure 15 also shows the conditional circular mean as a function of significant wave height. There does not appear to be any systematic variation around the overall mean value.

This figure also shows no observations of peak wave directions outside the range from 221° to 398° above a threshold peak significant wave height of 6 m; i.e. no observations in the range from 38° to 221°. Hence, we lack an empirical basis for assessing the effects of hurricanes in these directions, if they ever occur. Since we lack data to model the variation in the distribution of wave heights with direction, we assume that the omnidirectional distribution of peak significant wave heights, obtained above, applies uniformly to all directions. This assumption is expected to be conservative for directions in which hurricanes seldom occur, but may be un-conservative for the directions in which the most severe hurricanes do occur.

Three distribution functions are fitted to the wave directions in Figure 16: normal (Gaussian), Fourier series based [9] and Von Mises [8] distributions. The empirical densities are calculated for 30 degree wide bins, centred on the mean direction. In addition, interpolated points are included between adjacent directions, in order to allow a Fourier series of order 12 to be fitted without giving spurious maxima and minima. Although the Fourier series provided a useful distribution function for wave directions at Haltenbanken [10], it has a serious short-coming in the present case; viz. it has

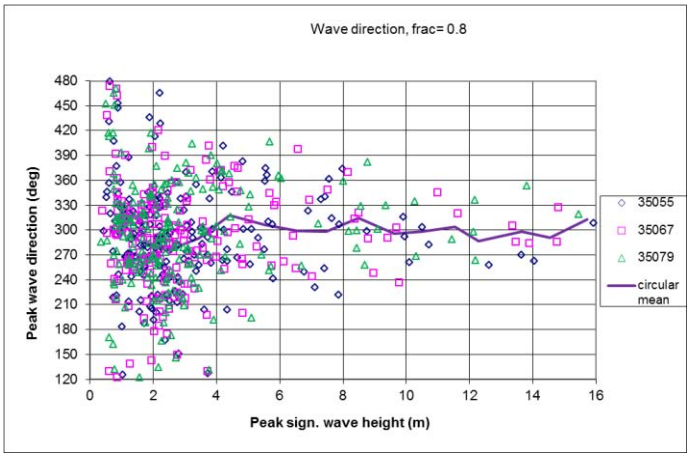

FIGURE 15 SCATTER PLOT OF PEAK WAVE DIRECTIONS AGAINST PEAK SIGNIFICANT WAVE HEIGHTS FROM 3 GRID POINTS.

difficulty with densities close to zero and can lead to illegal, negative densities. Two other distribution functions have been considered and both provide a reasonable fit to the data. A Von Mises distribution [8] is especially suitable for directional data , but is not included amongst the set of distributions available in PROBAN [11].

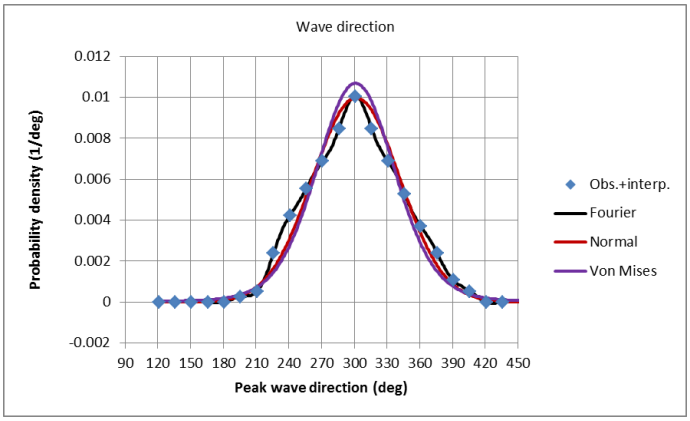

FIGURE 16 PROBABILITY DENSITY OF PEAK WAVE DIRECTIONS: EMPIRICAL DATA AND 3 FITTED DENSITY FUNCTIONS.

A normal distribution provides a simple, more practical alternative. The normal distribution is not ideal for directional data, because it has infinite tails which include repetitions of the same direction at intervals of 360°. However, this is not likely to lead to any problems in the present case, and a truncated normal distribution or a beta distribution can be applied in PROBAN if necessary.

It is suggested that the normal distribution be applied with a mean value of 301° and a conditional standard deviation, given (in degrees) as an exponential function of the peak significant wave height (in metres), with coefficients:

$a_0 = 9,\ a_1 = 152, a_2 = -0.186.$

Wind directions

The wind direction simultaneous with the peak wind speed during a hurricane is here referred to as the peak wind direction. The wind direction from which the wind is blowing (clockwise from true North) is taken from the hindcast data. It is converted to the direction towards which the wind is blowing by adding 180° and normalising the range. This is more convenient for comparison with the wave directions. Peak wind directions are extracted from the data set. Initial exploration of the data indicates that it can be useful to consider peak wind directions relative to peak wave directions. A scatter plot of relative wind directions against peak wind speeds is shown in Figure 17. The relative directions tend to be fairly small under severe conditions. The circular mean relative direction is -27° above the threshold level and there does not appear to be any systematic trend in the conditional, mean, relative directions. It is suggested that the normal distribution be applied with this mean value and a conditional standard deviation, given (in degrees) as an exponential function of the peak wind speed (in m/s), with coefficients:

$a_0 = 1,\ a_1 = 40.4, a_2 = -0.0095.$

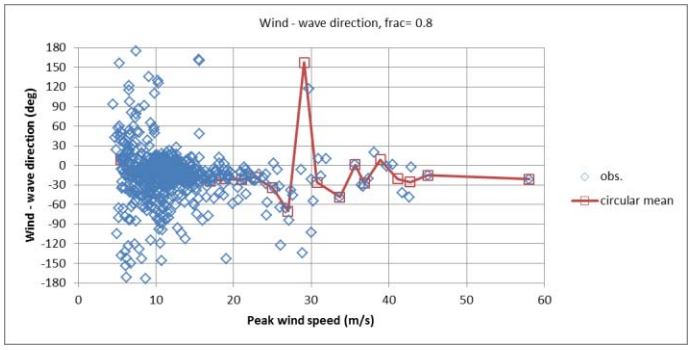

FIGURE 17 SCATTER PLOT OF WIND DIRECTION RELATIVE TO WAVE DIRECTION AGAINST WIND SPEED, FROM 3 GRID POINTS.

The data on peak wind directions represents the wind directions when the peak wind speed is registered at each grid point. These instantaneous wind directions may be very different from the overall direction of advance of the hurricane at that time, due to the rotation about the eye of the storm. If the right hand side of the hurricane passes through the grid point, then the peak wind direction will likely be close to the hurricane direction. If the left hand side of the hurricane passes through the grid point, then the peak wind direction may even be opposed to the hurricane direction. Furthermore, the peak wind speed is likely to be lower on the left hand side than on the right hand side. These features affect the distribution of wind directions and might be incorporated in a more advanced model for wind speeds and directions than is considered here.

Current directions

The current direction simultaneous with the peak current speed during a hurricane is referred to as the peak current direction. The vector average current direction is taken from the hindcast data, defined as the direction towards which the

current is flowing, taken clockwise from North. Exploratory analysis indicates that it is useful to model the peak current direction relative to the peak wind direction. A scatter plot of relative current directions against peak wind speeds is shown in Figure 18. A Gaussian distribution is recommended with mean value 74° and standard deviation 29° for the relative current direction.

This completes the description of the probabilistic hurricane model.

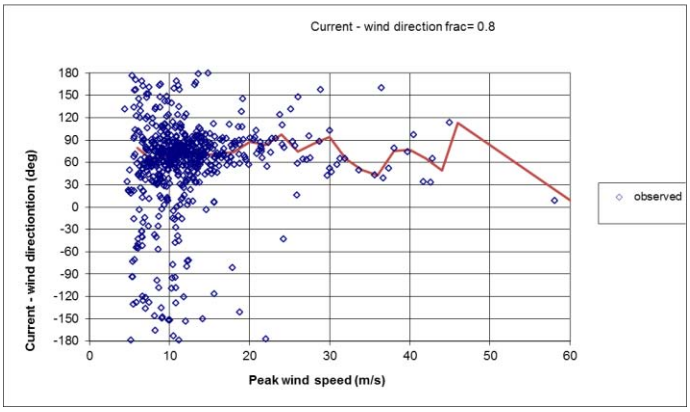

FIGURE 18 SCATTER PLOT OF PEAK CURRENT DIRECTION RELATIVE TO PEAK WIND DIRECTION AGAINST WIND SPEED, FROM 3 GRID POINTS.

TENSION DISTRIBUTION

Let the random vector Θ define hurricane conditions, with the components introduced above:

peak significant wave height, peak wind speed, peak current speed, peak wave direction, peak wind direction, peak current direction, linear shape coefficient for wave height (and current speed), linear shape coefficient for wind speed, rates of change for peak wave period, wave direction, wind direction and current direction, duration of waves above 80% of peak height, duration of wind above 80% of peak speed, lead time of peak wind before peak waves and lag of peak current after peak waves.

Given a realisation θ of this random vector, the shape functions may be applied to specify the set of n short-term, stationary conditions, each of 15 minutes duration, that make up that hurricane. This set of short-term conditions is denoted $\psi_i(\theta), i = 1, \dots, n$, where the vector ψ has the components:

significant wave height, wind speed, current speed, wave direction, wind direction, current direction and peak wave period.

The conditional, distribution of the extreme value of tension Z in a mooring line during such a 15-minute interval can be described by a Gumbel distribution

$$F_{Zi}\,(z;\theta,15\text{min}) = exp\{-\exp\big[-a_Z(\psi_i(\theta))\big(z - b_Z(\psi_i(\theta))\big)\big]\} \quad \textbf{(5)}$$

where the scale and location parameters a_Z, b_Z are determined for the applicable short-term conditions $\psi_i(\theta)$. The choice of 15 minutes for a stationary interval basically reflects the sampling interval of the data. It seems a reasonable choice with respect to the rates of change in Figure 1and Figure 2 and has not been investigated any further.

In practice, the tension distribution parameters are calculated in advance, for a large set of short-term conditions, intended to span the set of short term conditions arising in the hurricanes to be considered. Perhaps 5000 different short-term states may be considered. For each short term state, the response of the mooring line is simulated in the time domain and the maxima of the mooring line tension are extracted. A Weibull distribution is fitted to these maxima and the corresponding Gumbel distribution of 15-minute extreme tension is derived from the distribution of maxima. A response surface is used to interpolate on these results and provide the distribution parameters required in equation **(5)** for the specified short term conditions $\psi_i(\theta)$. This procedure is described in a little more detail in [10].

The conditional, extreme value distribution of tension in a specific hurricane is simply obtained by taking account of all the short-term intervals during that hurricane

$$F_Z\,(z;\theta,\text{hurricane}) = \prod_{i=1}^{i=n} F_{Zi}\,(z;\theta,15\text{min}) \quad \textbf{(6)}$$

Although adjacent intervals are conditional on the same hurricane, the conditional, short-term, extreme value distributions are independent in the sense required for equation **(6)**.

The marginal, extreme value distribution of tension in a random hurricane is then obtained by integrating with respect to the distribution of hurricane conditions

$$F_Z\,(z;\text{random hurricane}) = \int F_Z\,(z;\theta,\text{hurricane}) f_\Theta(\theta)\,d\theta \quad \textbf{(7)}$$

This integration is carried out using a second order reliability method (SORM), with the PROBAN program [12]. The first order reliability method (FORM) tends to be inaccurate when random directions are involved, while good results have been obtained with SORM [9], [10]. The joint probability density function of the hurricane conditions $f_\Theta(\theta)$ is simply obtained as the product of the appropriate marginal and conditional densities described above.

Finally, the frequency of hurricanes is taken into account, assuming a Poisson process, to obtain the extreme value distribution of line tension during t years as

$$F_Z\,(z;t\text{ years}) = exp\{-vt[1 - F_Z\,(z;\text{random hurricane})]\} \quad \textbf{(8)}$$

This equation is only applicable to fairly high tension levels, arising from hurricanes. Other conditions have to be taken into account for lower tension levels, and to account for loop current conditions.

SAMPLE RESULTS

Figure 19 to Figure 28 provide a detailed comparison of the hurricane model with hindcast data for the hurricane illustrated in Figure 1 and Figure 2. In this comparison, the model parameters estimated from this particular hurricane are used, rather than the randomised parameters. The time axis in the figures gives the time after the peak significant wave height.

Figure 19 to Figure 21 deal with the intensities of the 3 metocean effects: waves, wind and current. As intended, the model corresponds precisely to the hindcast data at the respective peaks of these effects. The separation in time of these peaks also corresponds precisely to the hindcast.

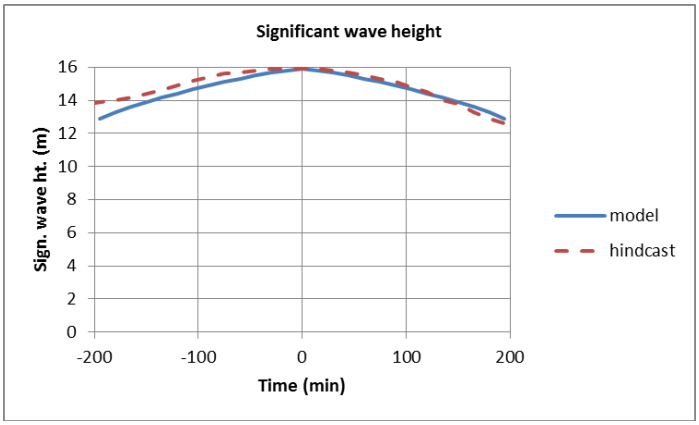

FIGURE 19 TIME VARIATION OF SIGN. WAVE HEIGHT AROUND PEAK OF HURRICANE IN FIGURE 1.

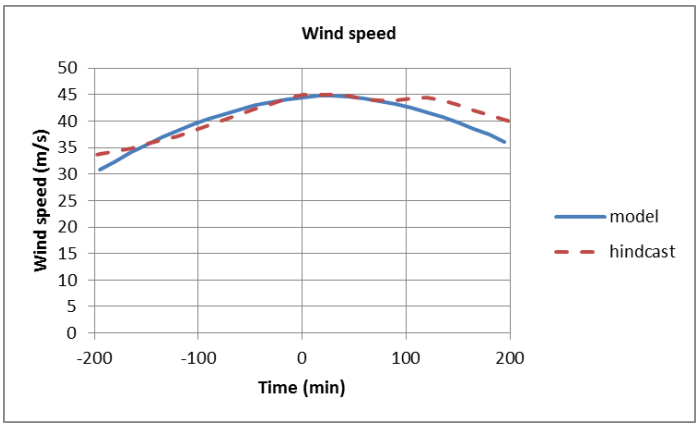

FIGURE 20 TIME VARIATION OF WIND SPEED AROUND PEAK OF HURRICANE IN FIGURE 1.

The model shape function (linear + parabola) provides a fair approximation to the time variation around the peaks, but some deviations are seen. In particular, the current speed is conservative. A modification was found necessary, because the initial intention to apply the shape function for wave height to current speed, with a time shift, was found to be excessively inaccurate. Hence, the shape function determined for current is applied instead – and the asymmetric shape of the actual time variation gives a conservative rising current speed when forced into a symmetric model. We intend to improve the shape function for current further by fitting it to the rising current alone, ignoring the shape of the falling current.

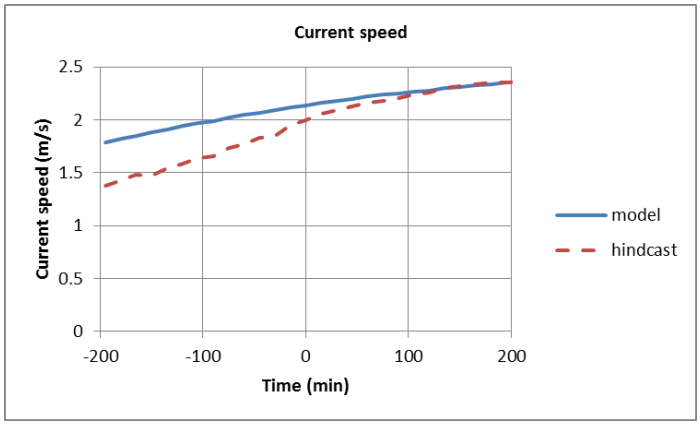

FIGURE 21 TIME VARIATION OF CURRENT SPEED AROUND PEAK OF HURRICANE IN FIGURE 1.

Figure 22 to Figure 24 deal with the time variation of the metocean directions. Again, the model directions of waves and wind agree precisely with the hindcast directions at peak waves and peak wind, respectively. A further modification of the current model is applied to make the model current direction agree with the hindcast at the peak wind speed, rather than at the peak current speed. This is intended to provide more accurate mooring line response around the peak wind and wave conditions. The linear model for variation of the directions provides good trends, but some deviation is present. The bilinear model for peak wave period performs well in Figure 25.

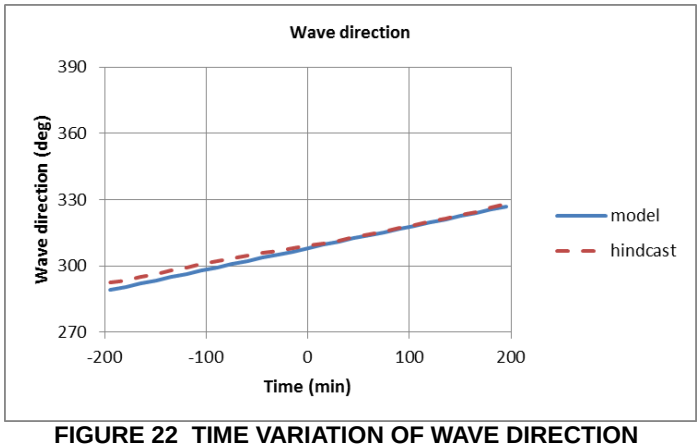

FIGURE 22 TIME VARIATION OF WAVE DIRECTION AROUND PEAK OF HURRICANE IN FIGURE 1.

A response surface for the distribution parameters of mooring line tension is applied to compare the response provided by the metocean model with the response provided by

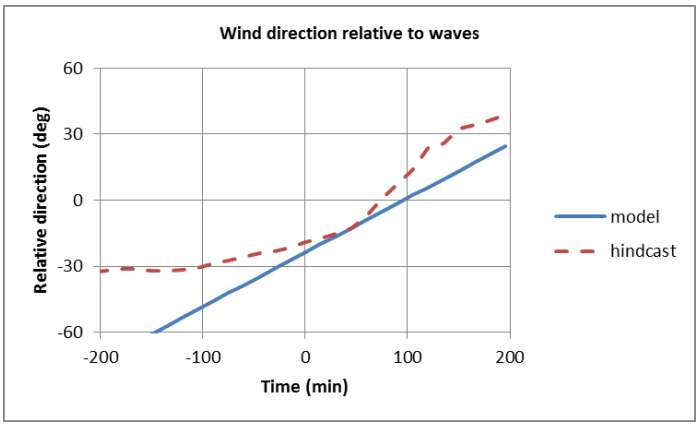

FIGURE 23 TIME VARIATION OF WIND DIRECTION AROUND PEAK OF HURRICANE IN FIGURE 1.

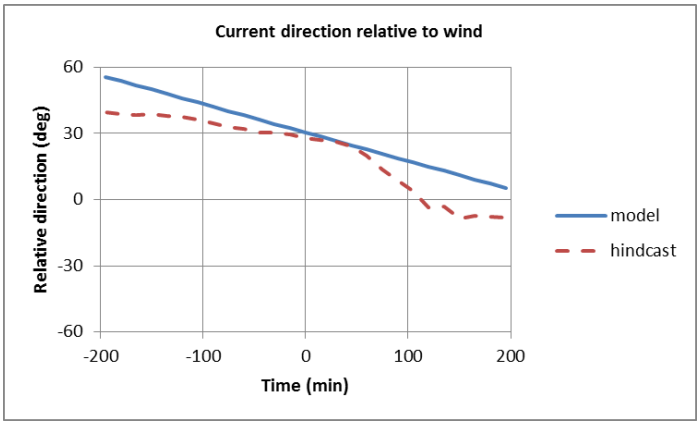

FIGURE 24 TIME VARIATION OF CURRENT DIRECTION AROUND PEAK OF HURRICANE IN FIGURE 1.

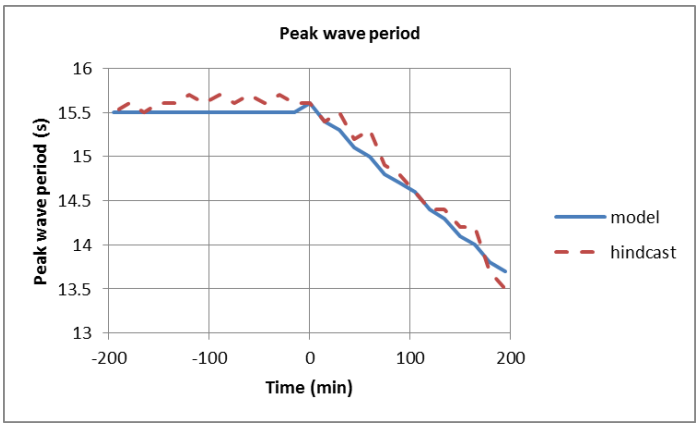

FIGURE 25 TIME VARIATION OF PEAK WAVE PERIOD AROUND PEAK OF HURRICANE IN FIGURE 1.

direct application of the hindcast data for this hurricane. A large, drilling semi-submersible in 1500 m water depth with 12 mooring lines in 4 clusters is used in the response calculations. Each mooring line has a chain-wire-chain configuration. The top chain has 76 mm diameter and a minimum breaking load of 6001 kN. The pretension is 1650 kN. One mooring line is considered, at the SE corner of the platform, with a direction of 121°, directly opposed to the mean wave direction of 301°. The mooring system is designed for a 10-year return period, with a significant wave height of 10.7m. Thus, it is inadequate for the present hurricane, but still provides a reasonably realistic response model, provided that the lines are assumed to be stronger than they really are, so the system remains intact in these conditions.

Parameters of the Gumbel distribution (equation **(5)**) for extreme line tension during 15 minutes exposure are retrieved from the response surface for the varying conditions during the hurricane and plotted in Figure 26 and Figure 27. The parameters derived from the metocean model agree quite well with the parameters derived from the hindcast conditions. The model seems to be slightly conservative. The extreme tension distribution for this hurricane is calculated from these parameters, according to equation **(6)** and shown in Figure 28. Reasonable agreement in tensions is obtained, with slightly conservative results from the metocean model.

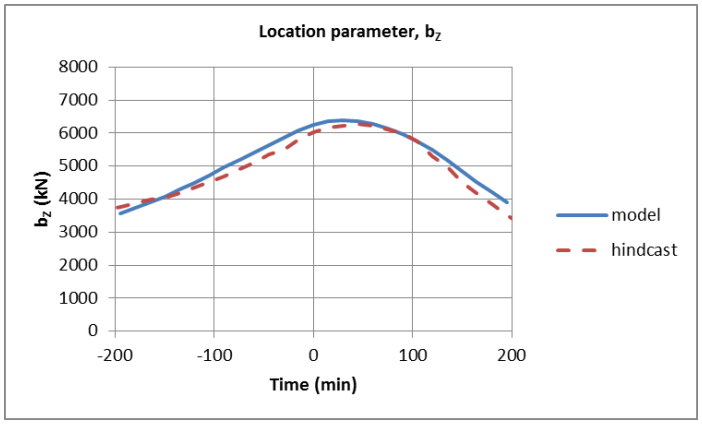

FIGURE 26 TIME VARIATION OF LOCATION PARAMETER FOR LINE TENSION AROUND PEAK OF HURRICANE IN FIGURE 1.

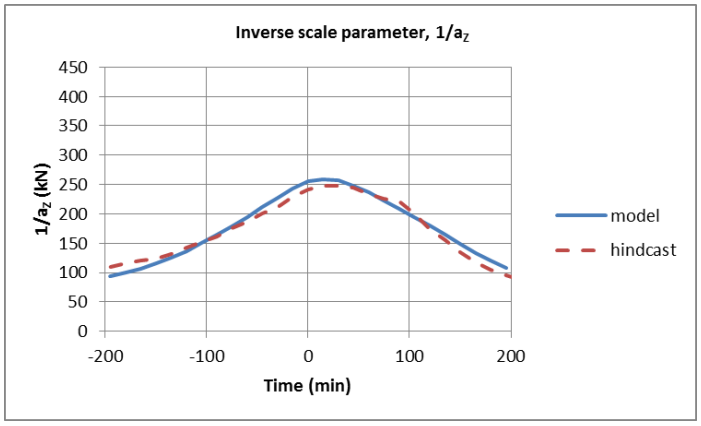

FIGURE 27 TIME VARIATION OF INVERSE SCALE PARAMETER FOR LINE TENSION AROUND PEAK OF HURRICANE IN FIGURE 1.

Comparisons have also been carried out for two other hurricanes, so far, which confirm the general trend of agreement between model and hindcast exhibited here.

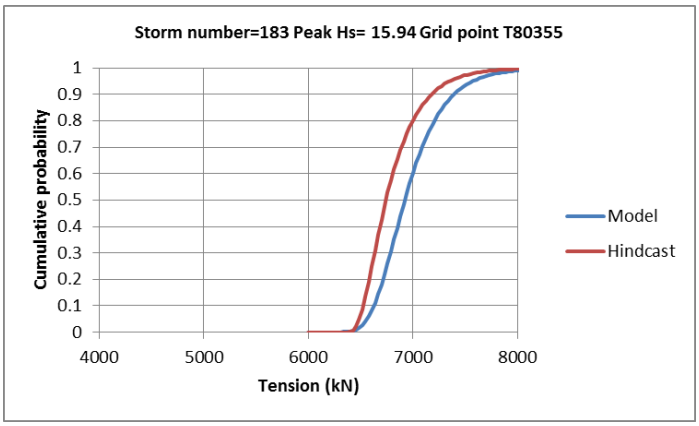

FIGURE 28 DISTRIBUTION OF EXTREME LINE TENSION DURING HURRICANE IN FIGURE 1.

Some checking of the chosen 80% portion has been carried out with these examples. Only the response analysis directly based on the hindcast is used and the analysed portion is gradually reduced in length. No significant change is seen in the response distribution for these cases if only the part of the hurricane above 90% of the peak height is included.

CONCLUSIONS

A probabilistic model for the variation of metocean conditions during a hurricane has been developed and fitted to data from one location in the Gulf of Mexico. The model includes salient aspects of the inter-dependency of the time histories of wave, wind and current effects. A linear plus parabolic shape function is used to model the time variation of the intensities of these effects in the vicinity of peak severity. The shape function is randomised.

The probabilistic metocean model allows extrapolation of hurricane conditions beyond the observed cases. This should be especially useful when there is a possibility of changes in the nature of system response with increased metocean severity. The model is intended for use in the reliability analysis of mooring lines, but should also be applicable to some other types of offshore response.

The probabilistic model includes a relatively large set of random variables. Further testing is necessary to confirm that the model is adequately accurate. Subsequently, it will be possible to explore the importance of the individual random variables. It seems likely that some of the random variables are less important and may be simplified as deterministic variables.

ACKNOWLEDGMENTS

This hurricane model has been developed within the NorMoor joint industry project, with the following participants: BP, Det norske oljeselskap, Statoil, GDF Suez Norge AS, Total, BG Norge Limited, Petrobras, Delmar, Vryhof, Single Buoy Moorings, APL, Transocean, Det Norske Veritas, Petroleum Safety Authority in Norway, Norwegian Maritime Directorate, UK Health and Safety Executive, Vicinay Cadenas, Ramnäs and Lankhorst Ropes. Permission to publish this paper is gratefully acknowledged. The material presented herein should not necessarily be taken to represent the views of these companies. Comments to the model from Øistein Hagen, Sverre Haver, Kjersti Bruserud and Richard Gibson are appreciated.

REFERENCES

[1] Larsen, K., Mathisen, J., (1996), "Reliability-Based Mooring System Design for a Drilling Semisubmersible," Proc. 6th Int. Offshore & Polar Engng. Conf., Los Angeles.

[2] Tromas, P., Vanderschuren, L., (1995), "Response Based Design Conditions in the North Sea: Application of a New Method," Offshore Technology Conf., paper OTC 7683, Houston.

[3] Wen, Y.K., (1988), "Environmental Event Combination Criteria, Phase I, Risk Analysis," Research report for the project PRAC-87-20, sponsored by API, Dept. Civil Engng., Univ. Illinois.

[4] Toro, G.R., Cornell, C.A., Cardone, V.J., Driver, D.B., (2004), "Comparison of Historical and Deductive Methods for the Calculation of Low-Probability Seastates in the Gulf of Mexico", 23rd Int. Conf. Offshore Mechanics & Arctic Engng., OMAE2004-51634, ASME, Vancouver.

[5] Oceanweather Inc., (2010), "GOMOS08: Gulf of Mexico Oceanographic Study 2008, Project Description," Cos Cob, Connecticut.

[6] Nataf,A., (1962) "Determination des Distribution dont les Marges sont Donnees," Comptes Rendus de l'Academie des Sciences, Paris, Vol 225, pp. 42-43.

[7] Bitner-Gregersen, E.M., Haver, S., (1989), "Joint Long Term Description of Environmental Parameters for Structural Response Calculation", 2nd Int. Workshop on Wave Hindcasting and Forecasting, Vancouver.

[8] Mardia, K.V., Jupp, P.E., (2000), "Directional Statistics," John Wiley & Sons Ltd, Chichester.

[9] Mathisen, J., Ronold, K.O., Sigurdsson, G., (2004), "Probabilistic Modelling for Reliability Analysis of Jackets," OMAE2004-51227, ASME, Vancouver.

[10] Mathisen, J., Okkenhaug, S., Larsen, K., (2011), "On the Probability Distribution of Mooring Line Tensions in a Directional Environment," OMAE2011-50104, ASME, Rotterdam.

[11] DNV Software, (2002), "Sesam User Manual, PROBAN Distributions, Continuous, Discrete and Correlated Distributions," DNV report no.94-7089, rev.2, Høvik.

[12] DNV Software, (2004), "Sesam User Manual, PROBAN, General Purpose Probabilistic Analysis Program" DNV report no.92-7049, rev.5, Høvik.

[13] Ronold, K.O., Winterstein, S.R., (1994), "Stochastic Storm Profiles for Strain Accumulation in Clay," ASME JOMAE Vol.116, pp.28-34.